Supporting Information

Folate Engineered Microvesicles for Enhanced Target and Synergistic Therapy towards Breast Cancer

Lian Zhu, [†] *Di Dong,* [†] *Zi-Li Yu,* [‡] *Yi-Fang Zhao,* [‡] *Dai-Wen Pang,* [†] *Zhi-Ling Zhang* [*,†]

†College of Chemistry and Molecular Sciences, Key Laboratory of Analytical Chemistry for Biology and Medicine (Ministry of Education), Wuhan University, Wuhan 430072, China.

‡School and Hospital of Stomatology, Key Laboratory of Oral Biomedicine (Ministry of Education) and Department of Oral and Maxillofacial Surgery, Wuhan University, Wuhan 430079, China.

Corresponding Author

*E-mail: zlzhang@whu.edu.cn

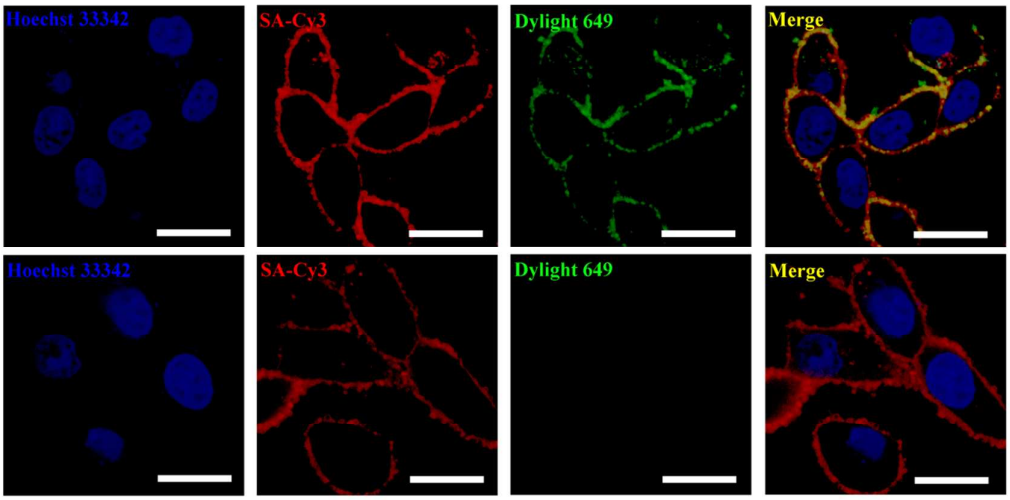

Fig. S1. Confocal microscope images of the Cal 27 cells. The first column referred to the cell nucleus, second column depicted the characterization of the biotin on the membrane, the third column displayed the modification of folate acid on the surface of the cell. the fourth column displayed the merged images. Scale bars referred to 10 μm.

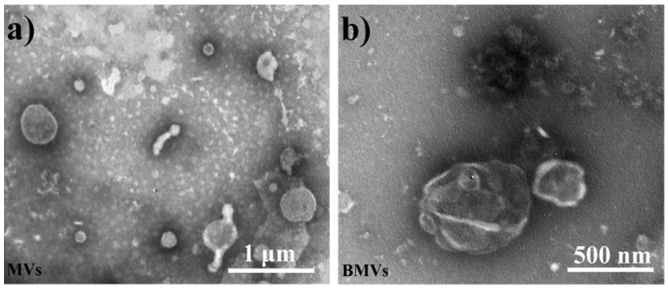

Fig. S2. TEM images of different formats of Cal 27 cell derived MVs. a, b) respectively referred to MVs and BMVs.

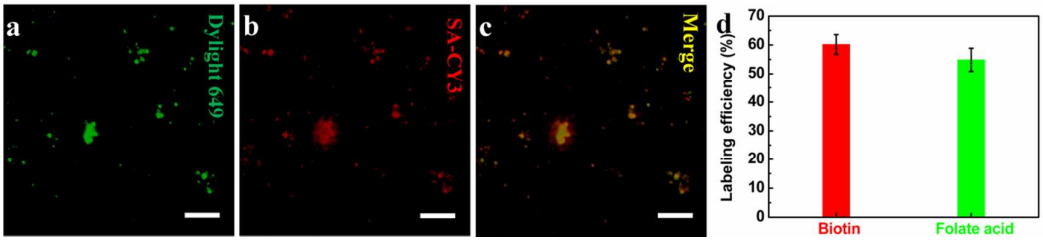

Fig. S3. Confocal microscope characterization of MVs. a-c) Confocal fluorescence images of the MVs engineered with biotin and folate acid. d) Modification efficiency of biotin and folate acid characterized with FCM.

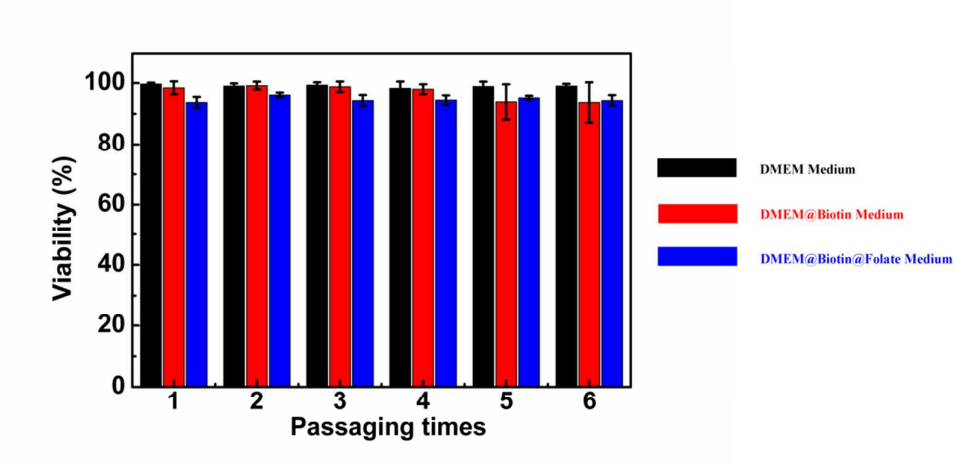

Fig. S4. Viability characterization of Cal 27 cells under different culture conditions.

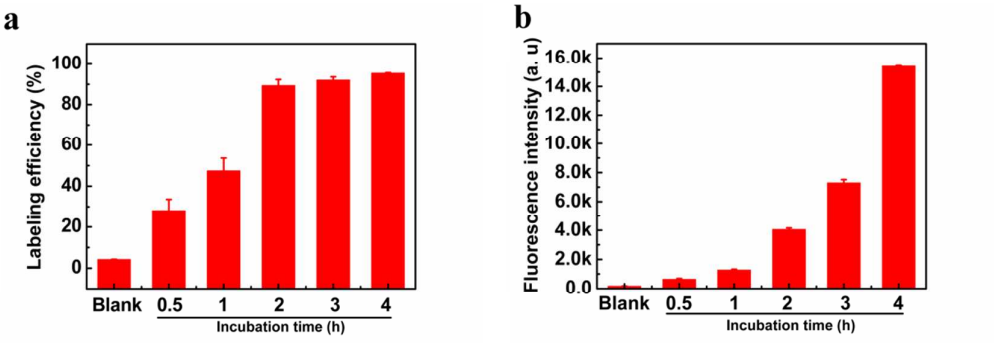

Fig. S5. FCM characterization of the DiO labeled BFMVs entering into MDA-MB-231 cells. a) Labeling efficiency altered with the increased incubation time, each for three duplicates. b) Fluorescence intensity versus the increased incubation time, each for three duplicates.

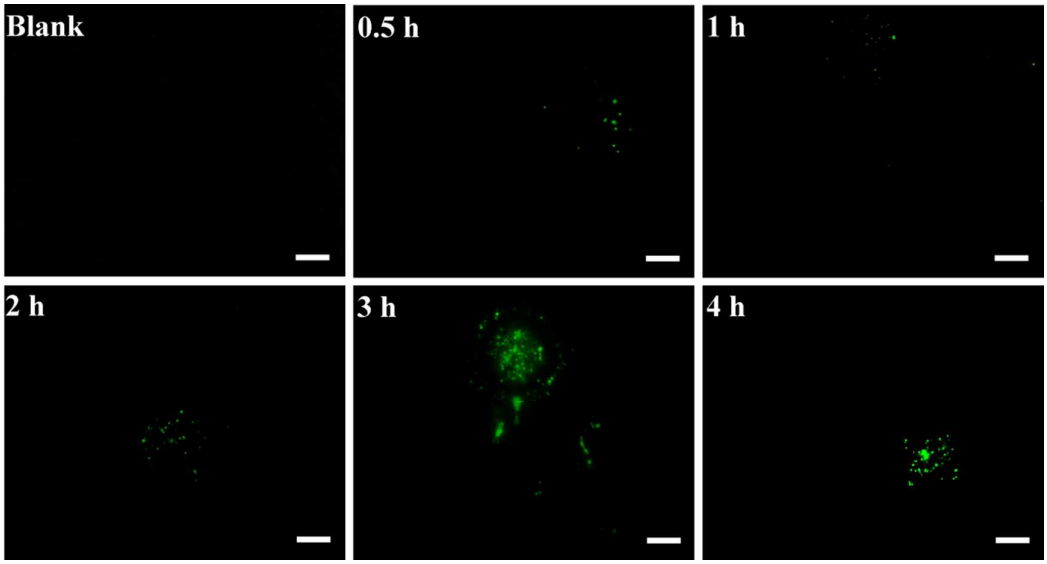

Fig. S6. Confocal characterization of the DiO labeled BFMVs entering into MDA-MB-231 cells under different incubation periods. The green particles referred to single BFMVs. Scale bars referred to 10 μm.

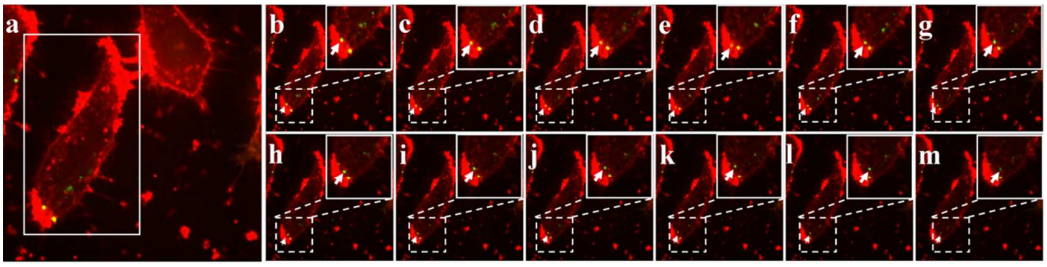

Fig. S7. Confocal microscopy for dynamic characterization of DiO labeled BFMVs entering into MDA-MB-231 cells. a) Panoramagram of the DiO labeled BFMVs entering into MDA-MB-231 cells. Movie S1 uploaded referred to the amplification of the square frame in Fig. S6a. b-m) Series of the captured images during the dynamic characterization of DiO labeled BFMVs entering into MDA-MB-231 cells. The cell membrane was labeled with CellMask^{TM}, white arrow in each image indicated the single DiO labeled BFMVs.

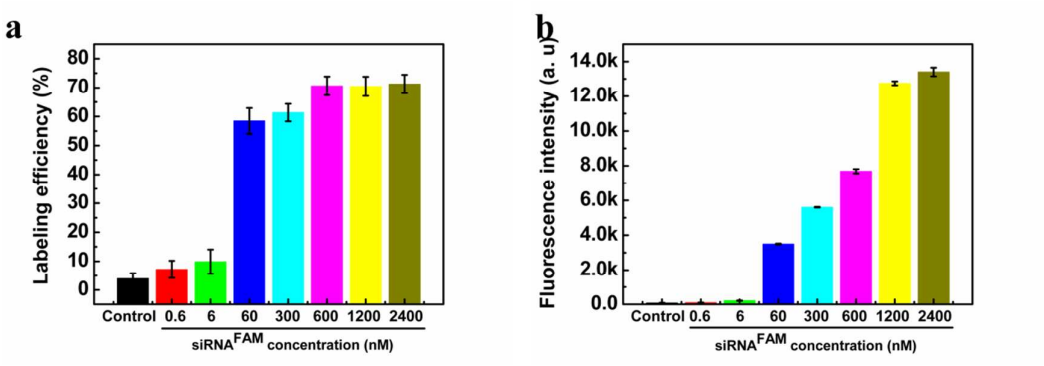

Fig. S8. Characterization of the package efficiency of FAM labeled Bcl-2 siRNA. a, b) Packaging efficiency and fluorescence intensity of the FAM labeled Bcl-2 siRNA packaged into BFMVs, each for three duplicates.

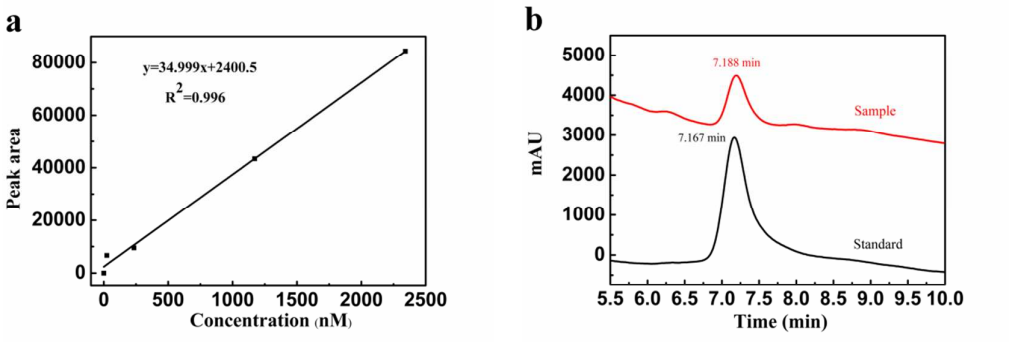

Fig. S9. HPLC characterization of the paclitaxel loading capability into BFMVs. a) Standard curve of paclitaxel. b) Chromatographic peaks of the standard sample and real sample.

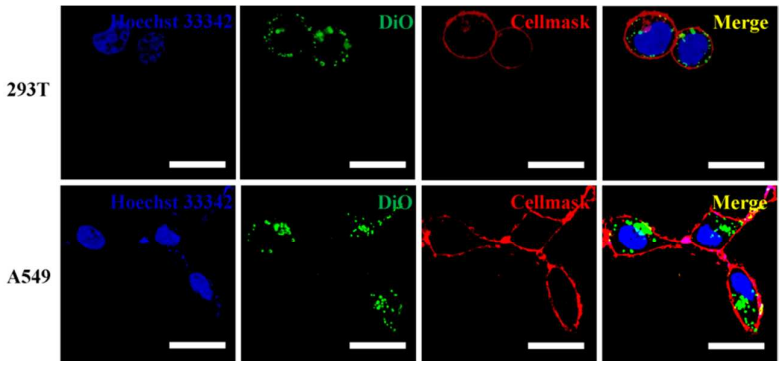

Fig. S10. Fluorescence images of the DiO labeled BFMVs entering into 293T and A549 cells, the blue, green and red channel referred to nucleus, BFMVs and cell membrane of 293T and A549 cells, respectively, scale bars referred to 10 μm.

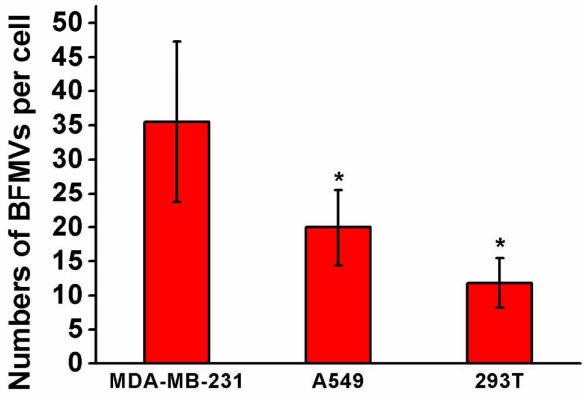

Fig. S11. Statistical data of the DiO labeled BFMVs entering into each cell.

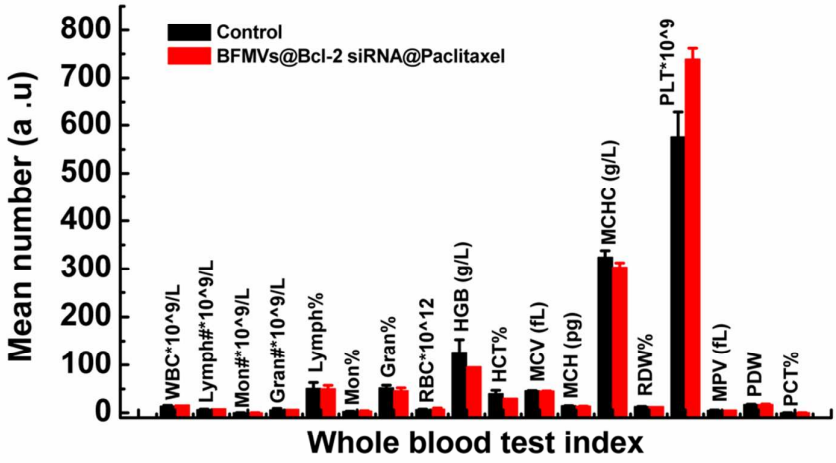

Fig. S12. Blood routine examination of the nude mice in the control and BFMVs@Bcl-2 siRNA@Paclitaxel group. From the left to the right referred to about the 18 blood index, the black and red columns respectively referred to control and experimental group, each for five duplicates.

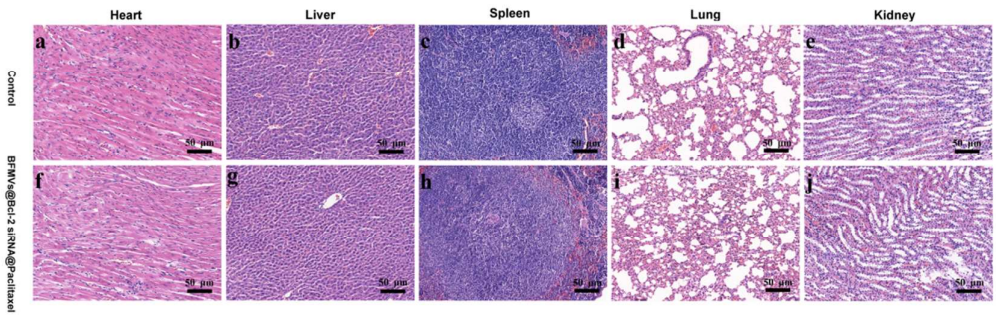

Fig. S13. HE staining of the main organs of the nude mice. a-e) and f-j) respectively represented the heart, liver, spleen, lung and kidney for the control and BFMVs@Bcl-2 siRNA@Paclitaxel group.

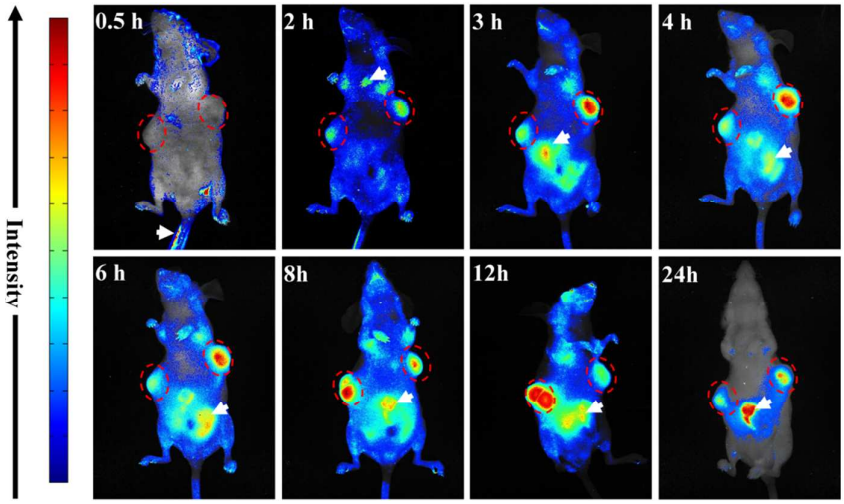

Fig. S14. Fluorescence images of the BFMVs labeled with SA-QDs in vivo. Oval in each image indicated the location of the BFMVs in tumor site. Arrow in each picture referred to the distribution of the BFMVs in vivo as the time elapsed.

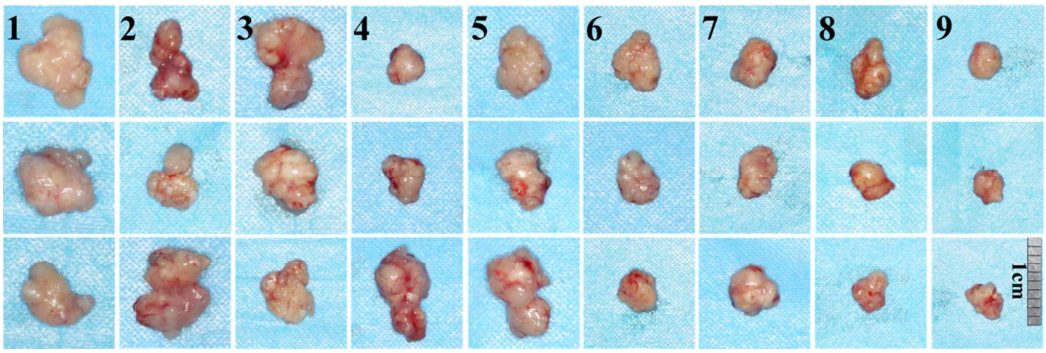

Fig. S15. Final relative tumor volume derived from the sacrificed nude mice. The Arabic numerals from 1 to 9 respectively referred to blank, BFMVs, Bcl-2 siRNA, paclitaxel, BFMVs@Bcl-2 siRNA, BFMVs@Paclitaxel, MVs@Bcl-2 siRNA@Paclitaxel, BMVs@Bcl-2 siRNA@Paclitaxel and BFMVs@Bcl-2 siRNA@Paclitaxel group, each for three duplicates in the same column.

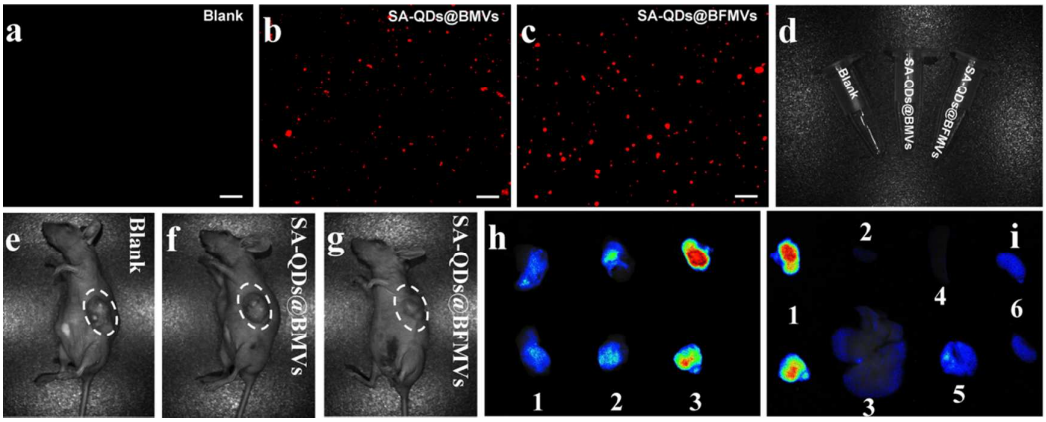

Fig. S16. Series characterization during the in vivo studies. a-d) Images of different formats of DDS samples. Scale bars referred to 10 μm. e-g) The images of nude mice in the three group during in vivo tumor imaging, the white circle referred to the tumor. h) Fluorescence images of the tumor during in vivo imaging, and 1, 2 and 3 respectively corresponded to blank, SA-QDs@BMVs DDS and SA-QDs@BFMVs DDS, each for double duplicates in the same column. i) Fluorescence images of the organs and tumor (1: tumor, 2: heart, 3: liver, 4: spleen, 5: lung, 6: kidney).

Table S1. Loading efficiency of paclitaxel characterized by HPLC.

N1 (nM)	M1 (μg)	N2 (nM)	M2 (μg)	PE (%)
300	0.13	60.4	0.026	80
600	0.26	206.6	0.09	65.4
1200	0.51	515.2	0.22	56.9
2400	1.02	594.9	0.25	75.5

Table S1. Loading efficiency of paclitaxel characterized by HPLC. N1, N2, M1, M2, PE respectively referred to initial concentration of paclitaxel, concentration of paclitaxel in the supernatant, initial total quantity of paclitaxel, and the total quantity of paclitaxel in the supernatant, the package efficiency of paclitaxel into BFMVs.

Table S2. All the sequences used in the research.

Primer	Sequences
Bcl-2	GAG GAU UGU GGC CUU CUU UTT(+) AAA GAA GGC CAC AAU CCU CTT(-)
GAPDH	GAG TCA ACG GAT TTG GTC GT(+) GAC AAG CTT CCC GTT CTC AG(-)
Negative control (Nc)	UUC UCC GAA CGU GUC ACG UTT(+) ACG UGA CAC GUU CGG AGA ATT(-)

Table S2. Main sequences used in the research.

Table S3. Intensity quantification of the band of western blot.

Number/intensity (a.u)	1	2	3
1	10534	14515	14657
2	11642	12086	11868
3	4857	5277	5008
4	4686	4690	4588
5	2611	2355	2457
6	4339	4049	3971

Table S3. Intensity quantification of the band of western blot. 1-6 in the left of the table S3 respectively represents Blank, BFMVs, BFMVs@Nc@Paclitaxel, BFMVs@GAPDH@Paclitaxel, BFMVs@Bcl-2 siRNA@Paclitaxel and BFMVs@Bcl-2 siRNA.